Approximative treatment of $5f$-systems with partial localization due to intra-atomic correlations

E. Runge and P. Fulde

Max-Plack-Institut für Physik komplexer Systeme, Nöthnitzer-Str. 38, 01187 Dresden, Germany

D. V. Efremov[*]

University of Groningen, Nijenborgh 4, 9747 AG Groningen, The Netherlands

N. Hasselmann

Institut für Physik, Johann-Wolfgang-Goethe Universität, 60054 Frankfurt am Main, Germany

G. Zwicknagl

*Institut für Mathematische Physik, Technische Universität Braunschweig,
Mendelssohnstr. 3, 38106 Braunschweig, Germany*

(Dated: February 2, 2008)

Increasing experimental and theoretical evidence points towards a dual nature of the $5f$ electrons in actinide-based strongly correlated metallic compounds, with some $5f$ electrons being localized and others delocalized. In a recent paper (PRB xxx, 2004), we suggested the interplay of intra-atomic correlations as described by Hund's rules and a weakly anisotropic hopping (hybridization) as a possible mechanism. The purpose of the present work is to provide a first step towards a microscopic description of partial localization in solids by analyzing how well various approximation schemes perform when applied to small clusters. It is found that many aspects of partial localization are described appropriately both by a variational wavefunction of Gutzwiller type and by a treatment which keeps only those interactions which are present in LDA+U calculations. In contrast, the energies and phase diagram calculated within the Hartree Fock approximation show little resemblence with the exact results. Enhancement of hopping anisotropy by Hund's rule correlations are found in all approximations.

I. INTRODUCTION

Many fundamental phenomena in solid-states physics can be considered as resulting from the competition of the repulsive Coulomb interaction trying to keep electrons as far from each others as possible and the kinetic energy term trying to delocalize electrons as much as possible. One of the most prominent examples is the Mott-Hubbard transition from a narrow-band metal with delocalized electrons to an insulator with localized electrons. Another one is band magnetism where the occupation of majority and minority bands differ dramatically. The resulting magnetic moment is typically aligned along certain crystallographic axes by an anisotropy energy which is much weaker than typical electronic energies given by the bandwidths. The recently suggested scenario of a dual nature of the $5f$ electrons in some uranium-based heavy-fermion compounds combines features of both these examples: There is experimental[1,2,3,4,5,6,7] and theoretical evidence[7,8,9,10,11,12,13,14] that in these materials some of the $5f$ electrons with $j = 5/2$ are localized and others are not. Which of the $5f$ orbitals form local moments and which form bands will depend on the geometry of the crystallographic environment of the particular actinide site, which leads to small differences of the hopping (hybridization) matrix elements.[15] Band struc-

ture calculations augmented by a mass-renormalization of the 'free' $5f$ electrons by crystal field excitations of the 'localized' $5f$ electrons lead to very good agreement of both areas and masses with dHvA data in UPt$_3$ and UPd$_2$Al$_3$.[8,11,12] In both cases, the best agreement was achieved treating the $j_z = \pm 3/2$ orbital as itinerant and including two f electrons in the ionic core. Calculations within the so-called LDA+U scheme[16] for UPd$_{3-x}$Pt$_x$ also suggest two fully occupied f electrons per U atom, however with $j_z = +5/2$ and $j_z = +3/2$ having occupations very close to unity.[13] A treatment within the self-interaction corrected local density approximation[17] (SIC-LDA) found for UPt$_3$ that the configurations of lowest energies have a local f^1 moment.[9] The same authors found for UPd$_2$Al$_3$ a groundstate characterized by the coexistence of localized f^2 and delocalized Uranium f electrons. Rare-earth metals and their sulfides, i.e., $4f$ electron systems, were also studied within the SIC-LDA and discussed in terms of localized and delocalized orbitals.[18] However, the physical reasoning is quite different from the present one.

In a recent paper,[14] we suggested the interplay of the intra-atomic correlations described by Hund's rules and a weakly anisotropic hopping as a possible mechanism leading to a separation of the $5f$ orbitals into band-forming and local-moment-forming ones. The underlying

idea can be described as follows. According to Hund's rules, atoms with three or two f electrons have angular momenta of $J = 9/2$ with 10-fold degeneracy and $J = 4$ with 9-fold degeneracy, respectively. Consider now transitions $M(j_z) = \langle 4J_z' | c_{j_z} | \frac{9}{2}J_z \rangle$ between any given pair of those degenerate states due to an annihilation operator c_{j_z} stemming from the kinetic energy term of the Hamiltonian. Obviously, these matrix elements depend strongly on j_z, leading to much larger transition amplitudes for some j_z than for others. Turning this argument around, the following scenario evolves: The largest product of the matrix elements $M(j_z)$ multiplied by the overlap t_{j_z} between the corresponding atomic wavefunctions of neighboring sites determine which pairs of $J = 9/2$ and $J = 4$ configurations are realized, thereby maximizing the corresponding energy gain. In most cases, the other hopping processes are then surpressed. This scenario is supported by exact diagonalizations of small clusters presented in Refs. 14 and 19.

This mechanism differs from other routes to partial localization and a dual nature in strongly correlated systems with degenerate d or f orbitals which were suggested, e.g., for manganites. For the latter, the physics is different: The degeneracy is split by strong crystal field with the lower t_{2g} orbitals forming a localized high-spin state while the e_g electrons are delocalized.

The numerical effort of exact cluster diagonalizations grows rapidly with system size. Any quantitative description of bulk material will necessarily involve some approximations. Over the last decades, considerable experience has been accumulated about the capability of various approximation schemes to describe many-body phenomena such as the above mentioned Mott-Hubbard transition and band magnetism.[20] The purpose of the present paper is to provide a first step towards a microscopic description of partial localization in solids by analyzing how various approximation schemes perform when applied to the cluster model of Ref. 14. The latter is briefly summarized in Sect. II. In Sect. III and IV, two widely used approximation schemes are applied. In the first, the Coulomb interaction is approximated by its diagonal part (direct term plus exchange term) in analogy with a modified local density approximation to density functional theory (LDA+U). The second scheme is mean-field theory, also known as the Hartree-Fock approximation (HF). In Sect. V, we study a variational wavefunction similar to that proposed by Gutzwiller in his famous paper on the ferromagnetism of transition metals.[21] We end in Sect. VI with a comparision of the various approximative treatments and with some tentative conclusions and speculations about the performance of these approximation schemes in bulk materials.

II. THE MODEL HAMILTONIAN

The simplest model describing the interplay between intra-atomic correlations of f electrons and weakly anisotropic hopping is considered in Ref. 14:

$$H = H_{\text{Coul}} + H_t + H_h. \tag{1}$$

The Coulomb interaction is written in terms of the usual fermionic operators $c_{j_z}^+(n)$ creating an electron on site n with angular momentum $j = 5/2$ and z component j_z as

$$H_{\text{Coul}} = \tag{2}$$
$$\frac{1}{2} \sum_n \sum_{j_{z1},\ldots,j_{z4}} U_{j_{z1}j_{z2}j_{z3}j_{z4}} c_{j_{z1}}^+(n) c_{j_{z2}}^+(n) c_{j_{z4}}(n) c_{j_{z3}}(n),$$

with Clebsch Gordon coefficients $C_{\cdots}^{\cdots}$ and Coulomb parameters U_J

$$U_{j_{z1}j_{z2}j_{z3}j_{z4}} = \left\langle j_{z1}j_{z2} | \hat{U} | j_{z3}j_{z4} \right\rangle \tag{3}$$
$$= \sum_J U_J C_{5/2,j_{z1};5/2,j_{z2}}^{JJ_z} C_{5/2,j_{z3};5/2,j_{z4}}^{JJ_z}.$$

The kinetic energy operator describes hopping (hybridization) between all pairs of neighboring sites $\langle nm \rangle$

$$H_t = - \sum_{\langle nm \rangle, j_z} t_{j_z} \left(c_{j_z}^+(n) c_{j_z}(m) + h.c. \right). \tag{4}$$

A ferromagnetic or antiferromagnetic external or internal field

$$H_h = - \sum_{n,j_z} h_n \, j_z \, c_{j_z}^+(n) c_{j_z}(n) \tag{5}$$

is included as well.

For the cases of two sites occupied by 5 electrons and for three sites and 8 electrons, iterative sparse-matrix diagonalization easily yields the respective ground states and some low-lying eigenstates. The sizes of the Hamilton matrices are 600×600 and $18,000 \times 18,000$, respectively, provided that site configurations are limited to f^2 and f^3 states, and 792×792 and $61,758 \times 61,758$ if this restriction is lifted.[19] For the sake of a transparent presentation, we focus in the present paper on the two-site model and stay in the 600 dimensional f^2-f^3 subspace.

The U_J parameters are more robust to changes in the chemical composition or the application of pressure than the the t_{j_z}. Thus, we use U_J parameters appropriate for UPt$_3$, $U_{J=4} = 17.21eV$, $U_{J=2} = 18.28eV$, $U_{J=0} = 21.00eV$,[8] and study the phase diagram in the t_{j_z} space. As in Ref. 14, we choose $t_{1/2} = t_{5/2}$ in the figures. The phase diagrams of the model Hamiltonian (1)-(4) obtained by exact numerical diagonalization is reproduced in Fig. 1.

III. DIAGONAL INTERACTION MATRIX ELEMENTS

Almost all electronic structure calculations for extended systems and large molecules are performed either in the framework of the local density approximation
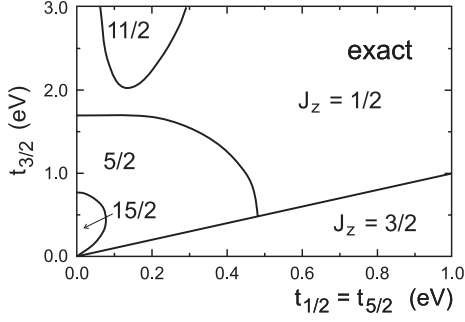
FIG. 1: Phase diagram for the f^2-f^3 model of Ref. 14 in the $t_{1/2}$-$t_{3/2}$ plane ($t_{5/2} = t_{1/2}$), derived from the total magnetization $\mathcal{J}_z$ (z component of the total angular momentum) of the ground state for infinitesimal field $h_n = 0^+$. Numbers indicate $\mathcal{J}_z$, which is a good quantum number.

FIG. 2: Phase diagram within the diagonal approximation (7) in the $t_{1/2}$-$t_{3/2}$ plane ($t_{1/2} = t_{5/2}$), derived from the total magnetization $\mathcal{J}_z$ of the ground state for infinitesimal field $h_n = 0^+$. In comparison with Fig. 1, note the different plot ranges.

(LDA) or using the Hartree-Fock approximation. The former accounts for correlations only in a rather crude way, while the latter neglects them altogether. Various recent papers suggested the inclusion of strong local correlations via an on-site energy-term of Hubbard type, $\sim U\hat{n}_j\hat{n}_k$, in LDA calculations within the LDA+U scheme[16] or the related SIC-LDA.[9,10,18] This is a promising route for some groundstate properties of highly correlated systems.

The key approximations of the LDA+U scheme are on the one hand the LDA itself and on the other hand the inclusion of only the diagonal interaction matrix elements (direct and exchange)

$$\tilde{U}_{j_{z_1} j_{z_2} j_{z_3} j_{z_4}} = (\delta_{j_{z_1} j_{z_3}} \delta_{j_{z_2} j_{z_4}} + \delta_{j_{z_1} j_{z_4}} \delta_{j_{z_2} j_{z_3}}) U_{j_{z_1} j_{z_2}, j_{z_3} j_{z_4}}. \quad (6)$$

The fact that this approximation corresponds to the LDA+U approach is best seen by inserting it into the Coulomb Hamiltonian (2) and rewriting the latter in terms of $\hat{n}_{a,j} = c_{a,j}^+ c_{a,j}$ as

$$\tilde{H}_{\text{Coul}} = \sum_{a=1,2} \sum_{j_z j_z'} \langle j_z j_z' | \hat{U} | j_z j_z' \rangle \, \hat{n}_{a j_z} \hat{n}_{a j_z'}. \quad (7)$$

Henceforth, we will refer to Eq. (7) as 'diagonal approximation.'

Figure 2 presents the resulting phase diagrams in the plane of hopping parameters $t_{1/2} = t_{5/2}$ and $t_{3/2}$. A visually striking difference to the result of the full calculation, Fig. 1, is the complete absence of the isotropic line $t_{1/2} = t_{3/2} = t_{5/2}$ in the phase diagram of the diagonal approximation to the Hamiltonian. This reflects the fact that the condition (6) of diagonality of $\tilde{U}$ with respect to z-component indices breaks rotational invariance. The z component of the total angular momentum remains a good quantum number. We note that the diagonal approximation overemphasizes the parameter space of phases with either strong ferromagnetic or strong antiferromagnetic alignment along z, i.e., $\mathcal{J}_z = 15/2$ and $\mathcal{J}_z = 1/2$. The simplified treatment quite correctly
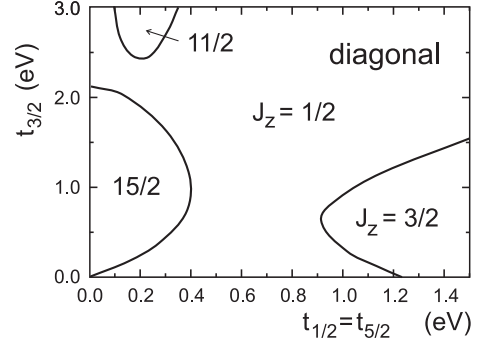
predicts the ferromagnetic 'high-spin' state $\mathcal{J}_z = 11/2$ for $t_{3/2} \gg t_{1/2} = t_{5/2}$. In general, the approximation fares worst in the case of small hopping anisotropy. The $\mathcal{J}_z = 5/2$ phase is missing, while a $\mathcal{J}_z = 3/2$ state is predicted only for rather strong hopping.

IV. HARTREE-FOCK APPROXIMATION

The Hartree-Fock approximation is one of the most widely used calculational approaches for interacting systems. For its implementation, one uses the single-particle density matrix

$$n_{a j_z, a' j_z'} = \sum_{\nu=1}^{N_{\text{tot}}} \varphi_{a j_z}^{(\nu)*} \varphi_{a' j_z'}^{(\nu)}, \quad (8)$$

written as sum of N_{tot} HF orbitals, which are superpositions of atomic orbitals described by the $c_{j_z}^+$

$$|\varphi^{(\nu)}\rangle = \sum_{a=1,2} \sum_{j_z=-5/2}^{5/2} \varphi_{a j_z}^{(\nu)} c_{j_z}^+ |0\rangle. \quad (9)$$

We impose no restrictions on the single-particle states, which are arbitrary combinations of angular momenta. The system of HF equations is[22]

$$E_\nu \, \varphi_{aj}^{(\nu)} = t_j \, \varphi_{\bar{a}j}^{(\nu)} + 2 \sum_{j'} v_{a,jj'}^{(HF)} \varphi_{aj'}^{(\nu)}, \quad (10)$$

with

$$v_{a,jj'}^{(HF)} = \sum_{kk'} n_{ak,ak'} \langle jk | \hat{U} | j'k' \rangle \quad (11)$$

and $a, \bar{a}$ denoting the two different sites. The two-particle matrix element $\langle jk | \hat{U} | j'k' \rangle$ comprises both the direct Hartree and the Fock contributions. Note that it is not

restricted to two pairwise equal indices in the j_z basis. The total energy is obtained from

$$E_{\text{total}} = \sum_\nu E_\nu - \frac{1}{2} \sum_\nu \sum_{jj'} \varphi_j^{(\nu)*} v_{a,jj'}^{(HF)} \varphi_{j'}^{(\nu)}, \quad (12)$$

where double-counting of the interaction energy is avoided in the usual way.[22]

In general, the HF solutions do not have the total $\mathcal{J}_z$ as a good quantum number. Therefore we cannot always use different $\mathcal{J}_z$'s to classify different phases. However, one still finds discontinuous jumps either of the expectation value $\langle \mathcal{J}_z \rangle$ or of its derivatives with respect to t_{j_z} or h and we use these to define phase boundaries. Moreover for some phases with small kinetic energy, self-consistent solutions $\varphi^{(\nu)}$ with good quantum numbers j_z are found and, thus, $\mathcal{J}_z$ is a good quantum number in those cases. This applies to the phases with $\mathcal{J}_z = 15/2$ and $17/2$. For larger hopping parameters, one finds in general continuous variations of $\langle \mathcal{J}_z \rangle$. We denote phases as 'AM' or 'FM' indicating antiferromagnetic or ferromagnetic spin correlations, respectively. Half-integer-valued subscripts give the approximate $\langle \mathcal{J}_z \rangle$ expectation value found for t_{j_z} parameters not too close to the phase boundaries.
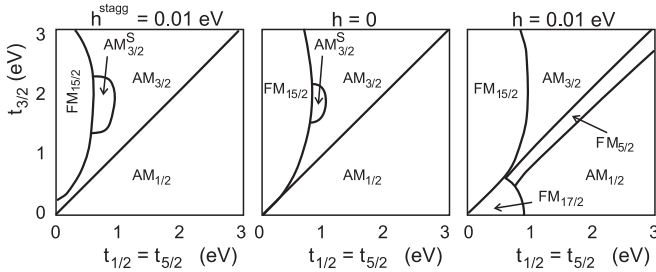

FIG. 3: Phase diagram in the $t_{1/2}$-$t_{3/2}$ plane (with $t_{1/2} = t_{5/2}$) in the Hartree-Fock approximation with ferromagnetic (right), vanishing (middle), and antiferromagnetic (left) fields. The phases are characterized from the z components of the angular momentum and the state occupation and labled according to the notation of Fig. 4 and 5.

Overall, the Hartree-Fock $t_{1/2}$-$t_{3/2}$ phase diagram in Fig. 3 shows only weak resemblance with the one from the exact calculation. The isotropic line is a phase boundary at zero field.

Figure 4 illustrates the occupation pattern of four important phases occuring in the phase diagrams shown in Figs. 1-3 and 7 of the present work as well as Fig. 5 of Ref. 14. A large angular momentum as implied by Hund's rules is obtained if electrons occupy preferentially states with either large positive or large negative angular momentum projections j_z – of course subject to the Pauli principle. Occupation of states with large positive or negative angular momentum projections is favored also by local (molecular) magnetic fields. In particular, the antisymmetrized product states $\left| \pm\frac{5}{2}, \pm\frac{3}{2}, \pm\frac{1}{2} \right\rangle \times \left| \pm\frac{5}{2}, \pm\frac{3}{2} \right\rangle$ minimize simultaneaously the Coulomb energy

and the magnetic energy. For not too strong hopping, the two sites (anti-)align their angular momenta in a (anti-)ferromagnetic field configuration, see left (right) column of Fig. 4.
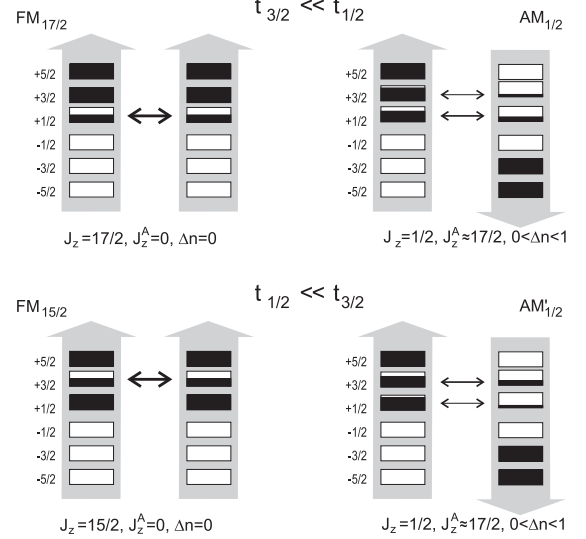

FIG. 4: Configurations relevant for weakly anisotropic hopping (hybridization) in the presence of ferromagnetic (FM, left column) and antiferromagnetic (AM, right column) fields for $t_{3/2} \ll t_{1/2} = t_{5/2}$ (top row) and $t_{1/2} = t_{5/2} \ll t_{3/2}$ (bottom row). Rectangles symbolize the j_z orbitals on both sites, with black areas presenting their occupation. The thickness of horizontal arrows between orbitals symbolizes their contributions to the kinetic energy gain. The arrow-shaped background emphasizes the role of the fields. Note the charge disproportionation $0 < \Delta n_f < 1$ in the antiferromagnetically aligned states.

Two crucial differences between FM and AF fields are obvious: (i) As drawn, in the FM case both sites have an f occupation $n_f = 2.5$, whereas in the AM case a small charge disproportionation $\Delta n_f < 1$ can be present. The AM configurations of Fig. 4 are, of course, degenerate due to the symmetry with respect to a simultaneous exchange of site index and $j_z \leftrightarrow -j_z$.

(ii) The FM and AM cases differ with respect to a possible quantum phase transition when going from $t_{3/2} < t_{1/2}$ to $t_{3/2} > t_{1/2}$ (compare in Fig. 4 the upper row with the lower row). In the AF case, with increasing $t_{1/2}$ the $j_z = 1/2$ electron starts to fluctuate more between the sites, whereas the $j_z = 3/2$ electron fluctuates less. This is a continuous cross-over, which however takes place rather suddenly because $j_z = 1/2$ fluctuations imply charge fluctuations which then suppress $j_z = 3/2$ fluctuations, and vice versa. In a level diagram such as the inset of Fig. 4 in Ref. 14, this corresponds to an avoided crossing.

In contrast, in the FM case one of $j_z = 1/2$ or $j_z = 3/2$ is not fully occupied. The transition is not a cross-over, but a simple level crossing with discontinuous change of

$\mathcal{J}_z$ and orbital occupation. This difference between sharp discontinuities on the FM side and smooth cross-overs on the AF side will be seen repeatedly in this work. We will see below that within the Hartree-Fock approximation the states $FM_{15/2}$, $FM_{17/2}$, and $AM_{1/2}$ dominate indeed in the phase diagram for finite fields and not too large hopping.

One further cautionary remark is in place: The representation in Fig. 4 shows only the occupation pattern, but does not reflect the correlations between different configurations.

Strongly anisotropic hopping $t_{3/2} \gg t_{1/2}$ lead in the full solution to $FM_{15/2}$, i.e. to ferromagnetic correlations and single occupancy of the binding $j_z = +\frac{3}{2}$ state. The corresponding wavefunction

$$|\Psi\rangle_{\frac{15}{2}} = \frac{c^+_{3/2}(a) + c^+_{3/2}(b)}{\sqrt{2}} c^+_{5/2}(a) c^+_{1/2}(a) c^+_{5/2}(b) c^+_{1/2}(b) |0\rangle \tag{13}$$

is a simple Slater determinant. Thus, it is not surprising that HF works well for this case. The parameter space of the $FM_{15/2}$ phase is, however, much larger in the HF approximation than in the exact calculation. It shrinks with increasing antiferromagnetic field and increases with increasing ferromagnetic field.

Outside the ferromagnetic phases in Fig. 3, the correlations are antiferromagnetic and $\langle \mathcal{J}_z \rangle \lesssim 3/2$. A kink separates a phase with $\langle \mathcal{J}_z \rangle \approx 1/2$, visualized in Fig. 4 as $AM_{1/2}$, from a phase with $\langle \mathcal{J}_z \rangle \approx 1$ at or near the isotropic line and $\langle \mathcal{J}_z \rangle \sim 3/2$ at larger values of $t_{3/2}$ which is denoted by $AM_{3/2}$ in Fig. 5. In a small bubble bordering the ferromagnetic $FM_{15/2}$ phase, a phase exists which we denote by $AM^S_{3/2}$, see Fig. 5. It can be considered as the symmetrized version of $AM_{3/2}$. The binding linear combinations with $j_z = +3/2$ and $j_z = -3/2$ are both half occupied and contribute equally to the kinetic energy gain by hopping (hybridization). Strongly anisotropic hopping with $t_{1/2} \gg t_{3/2}$ leads to $AM_{1/2}$, i.e. to an antiferromagnetic arrangement with broken left-right symmetry, i.e., $0 < \Delta n_f \lesssim 1$.

A region of maximal ferromagnetic moment ($FM_{17/2}$) is found for a ferromagnetic field which is still weak compared to the bare hopping strengths. For larger fields, the ferromagnetic phase $FM_{5/2}$ with 'intermediate' spin is found close to isotropic line. In this phase, all five electrons contribute to the kinetic energy gain.

Figure 5 shows also a phase denoted by $FM_{11/2}$, which is of overall ferromagnetic nature but dominated by $t_{3/2}$ hopping. It appears in Fig. 1 and 2 as well as in Fig. 8 below.

A. Partial localization

In order to quantify the degree of localization of a given j_z orbital by local correlations, we study the ratio of the j_z-projected kinetic energy T_{j_z} and the bare matrix ele-
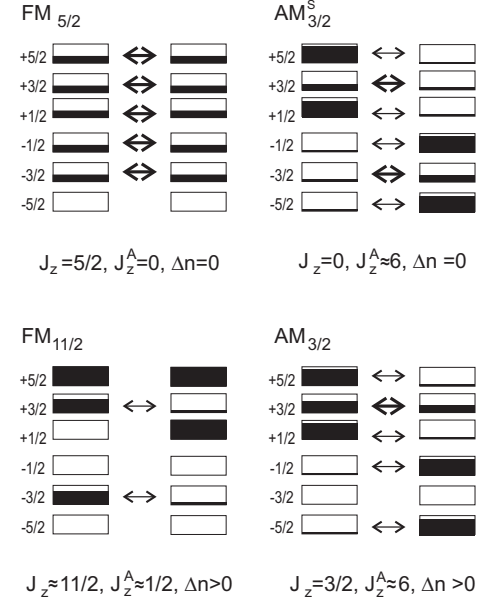

FIG. 5: Configurations relevant for large hopping: The upper left panel ($FM_{5/2}$) shows an overall ferromagnetic arrangement with all electrons contributing to the kinetic energy gain. The upper right panel ($AM^S_{3/2}$) presents an overall antiferromagnetic arrangement dominated by $t_{3/2}$ hopping which is symmetric with respect to the site index. $t_{3/2}$ hopping dominates also in the lower row. In the lower left panel ($FM_{11/2}$), the overall arrangement is of ferromagnetic type, whereas in the lower right panel ($AM_{3/2}$) it is of antiferromagnetic character. As in Fig. 4, black areas symbolize the orbital occupation and the linewidth of the arrows symbolize the corresponding contributions to the kinetic energy gain. Field directions are not indicated, in order to emphasize the role of the hopping for the formation of these states.

ment t_{j_z}[14]

$$\frac{T_{j_z}}{t_{j_z}} = \sum_{\langle nm \rangle, \pm} \langle \Psi_{gs} | (c^+_{\pm j_z}(n) c_{\pm j_z}(m) + h.c.) | \Psi_{gs} \rangle, \tag{14}$$

with $-2 \leq T_{j_z}/t_{j_z} \leq +2$ for two sites. A small ratio T_{j_z}/t_{j_z} indicates partial suppression of hopping for electrons in the $\pm j_z$ orbitals. For all cases considered in Ref. 14, we found small ratios of T_{j_z}/t_{j_z} for the smaller t_{j_z}, and values close to one or two for the dominant hopping matrix element.

In Fig. 6, we study the same quantity for the Hartree-Fock solutions. Again if $t_{3/2} \gg t_{1/2}, t_{5/2}$, ratios close to one are found for $T_{3/2}/t_{3/2}$, but much smaller values for $(T_{1/2} + T_{5/2})/t_{1/2}$, and vice versa. At first glance, this may look surprising since the Hartree-Fock method can not describe the correlations underlying the dual nature of the f electron in our model system. A closer look reveals that the correlations are simulated by symmetry breaking, i.e. by driving the corresponding occupations close to zero or two. In contrast, the full solution shows a reduced hopping also for intermediately occu-

pied orbitals. We conclude that HF mimics correlations by overemphasizing occupation differences. Thus, further studies are needed to gauge the usefulness of HF for bulk systems with partially localized $5f$ electrons.
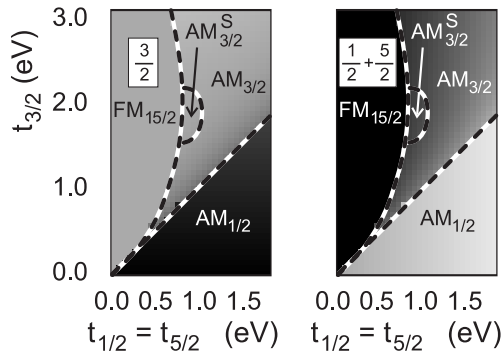

FIG. 6: Ratio (a) $T_{3/2}/t_{3/2}$ and (b) $(T_{1/2} + T_{5/2})/t_{1/2}$ in the Hartree-Fock approximation in the $t_{1/2}$-$t_{3/2}$ plane (with $t_{1/2} = t_{5/2}$ and $h_n = 0^+$) given as gray-scale plot (black: 0, white: 1.5). Phase boundaries of the middle panel of Fig. 3 are included for orientation.

B. Hartree-Fock with j_z eigenstates (UHF)

If the variational HF space is reduced further by requiring j_z-diagonal density matrices and self-consistent potentials

$$v_{a,j}^{(UHF)} = \sum_k n_{a,k} \langle jk|\hat{V}|jk\rangle, \qquad (15)$$

the z axis plays a special role (quantization axes), as it did in Sect. III, and the spherical symmetry is broken. Following the usual nomenclature, we refer to this approximation which allows different orbitals for different angular momenta but prescribes angular momenta as orbital quantum number, as the unrestricted Hartree-Fock (UHF)[22] – even though the wavefunction space is restricted in comparison to Eq. (9). The resulting phase diagrams, Fig. 7, are not identical, but close to those of the full HF solution in Fig. 3. Not surprisingly, the isotropic line does no longer play a special role. The corresponding phase boundary has moved to higher $t_{3/2}$ values, a consequence of the variational restriction favoring the maximally antiferromagnetic alignment with $\mathcal{J}_z = 1/2$.

Note that $\mathcal{J}_z$ is now a good quantum number. In particular, the border between $AM_{3/2}$ and $AM_{1/2}$ is here easily identifiable, the kink being replaced by a jump. A noticeable difference between the HF and the UHF phase diagram is that $AM_{3/2}^S$, i.e. the symmetrized version of $AM_{3/2}$, can not be found within the UHF approximation, because all six j_z values are partially occupied in this phase, cf. Fig. 5.

As an aside, we remark that numerical convergence in solving the restricted equation (15) is obtained in a small fraction of the time needed for solving the HF equations (8), (11).
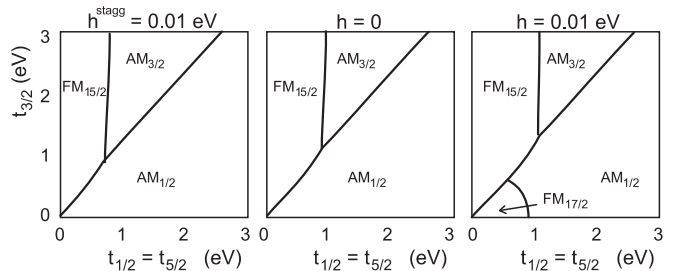

FIG. 7: Hartree-Fock approximation with variational space restricted to j_z eigenstates (UHF): Phase diagram in the $t_{1/2}$-$t_{3/2}$ plane ($t_{1/2} = t_{5/2}$) with ferromagnetic (right), vanishing (middle), and antiferromagnetic (left) fields. The phases are chararacterized from the z components of the angular momentum and the state occupation, cf. Fig. 4 and 5.

C. Charge disproportionation

The Hartree-Fock phase diagram is surprisingly rich with several phases showing charge disproportionation, i.e. a finite expectation value $0 < \Delta n_f < 1$ of the difference of site occupations. Note in particular the phase boundary in Fig. 3 between the closely related phases $AM_{3/2}$ and $AM_{3/2}^S$ at vanishing or staggered field.

The exact groundstates of the small cluster does not show charge disproportionation, because a suitable superposition of the two symmetry-related configurations will lead to a finite energy gain, completely analogous to the absence of ferromagnetism in small clusters at vanishing external fields. However, in both cases the energy gain can be extremely small if the configurations are sufficiently different. This feature of the numerically exact small cluster solution will often not survive the thermodynamic limit. In contrast, mean-field approaches easily lead to symmetry-broken solutions even for small clusters. This is so, because they reduce charge fluctuations and therefore simulate the effect of electron correlations. When symmetry breaking is experimentally observed in bulk samples it is overemphasized in a Hartree-Fock treatment. Thus, we take the trend of the HF solution towards charge disproportionation only as a hint that it might be worthwhile to look for, e.g., phase transitions driven by charge ordering in systems with partially localized $5f$ orbitals.

V. GUTZWILLER'S WAVEFUNCTION

The exact groundstates found in Ref. 14 often have a large overlap with a Gutzwiller-type wavefunction[21] of

the form

$$\left| \Psi_G \right\rangle = \hat{\mathcal{P}}_{f^2 f^3} \prod_{\nu=1}^{5} \tilde{c}_\nu^+ \left| 0 \right\rangle , \qquad (16)$$

where the projector $\hat{\mathcal{P}}_{f^2 f^3}$ retains only local f^2 and f^3 configuration. The single-particle orbitals generated by the $\tilde{c}_\nu^+$ are subject only to the orthogonality requirement. In most actual applications of the Gutzwiller ansatz, simple trial wavefunction are used for the single-particle states, e.g., the non-interacting, possibly polarized, Fermi sea. Here, we use the ansatz that each orbital has j_z as a 'good quantum number,' i.e.

$$\left| \Psi_G \right\rangle = \hat{\mathcal{P}}_{f^2 f^3} \prod_{\nu=1}^{5} \left(\cos\theta_\nu c^+_{j_z^{(\nu)}}(a) + \sin\theta_\nu c^+_{j_z^{(\nu)}}(b) \right) \left| 0 \right\rangle , \qquad (17)$$

with variational parameters θ_ν. Both, the numerator and the denominator of the energy expectation value

$$E[\{j_z^{(\nu)}\}, \{\theta_\nu\}] = \frac{\langle \Psi_G \mid H \mid \Psi_G \rangle}{\langle \Psi_G \mid \Psi_G \rangle} \qquad (18)$$

are polynomial expression in $\cos\theta_\nu$ and $\sin\theta_\nu$. Note that in the case of double occupancy $j_z^{(\nu_1)} = j_z^{(\nu_2)}$ the corresponding variational parameters θ_ν drop out of Eq. (18).

We performed numerical minimizations with respect to both the occupation pattern $\{j_z^{(\nu)}\}$ and the set of parameters $\{\theta_\nu\}$. In practice, the expectation value (18) is obtained explicitly from the Hamilton matrix in the many-particle site-spin representation (600×600) in terms of θ_ν. Then MATHEMATICA's implementation of Brent's algorithm is used for 1-dimensional, 3-dim., and 5-dim. numerical minimization in the case of 2, 1 and 0 doubly occupied angular momenta j_z, respectively. Even the five-dimensional minimum search is fast. Unfortunately, many occupation pattern have to be tried and different random initial conditions yield different answers. This makes an additional loop over various initial conditions necessary.

The obtained phase diagram is reproduced in Fig. 8a. Again, $\mathcal{J}_z$ is a good quantum number because the corresponding operator commutes with $\hat{\mathcal{P}}_{f^2 f^3}$. Both panels show a transition from a strongly polarized $\mathcal{J}_z = 15/2$ phase to the state of lowest possible polarization, i.e., $\mathcal{J}_z = 1/2$. A small pocket with $\mathcal{J}_z = 17/2$ is found at finite field. The phase diagram for small antiferromagnetic fields (not shown) is close to that for vanishing field with the high-spin phase $\mathcal{J}_z = 15/2$ being slightly reduced. As in the exact solution and in all other approximation schemes, the energy varies continuously (not shown).

The phase diagram of the Gutwiller wavefunction (17) is remarkably close to the exact diagonalization of the Hamiltonian keeping only diagonal matrix elements ('LDA+U') in Sect. III. We will see below that this is true for the total energies as well. This should not come as an surprise, because both approaches effectively reduce charge fluctuations but do not include angular correlations equally well.
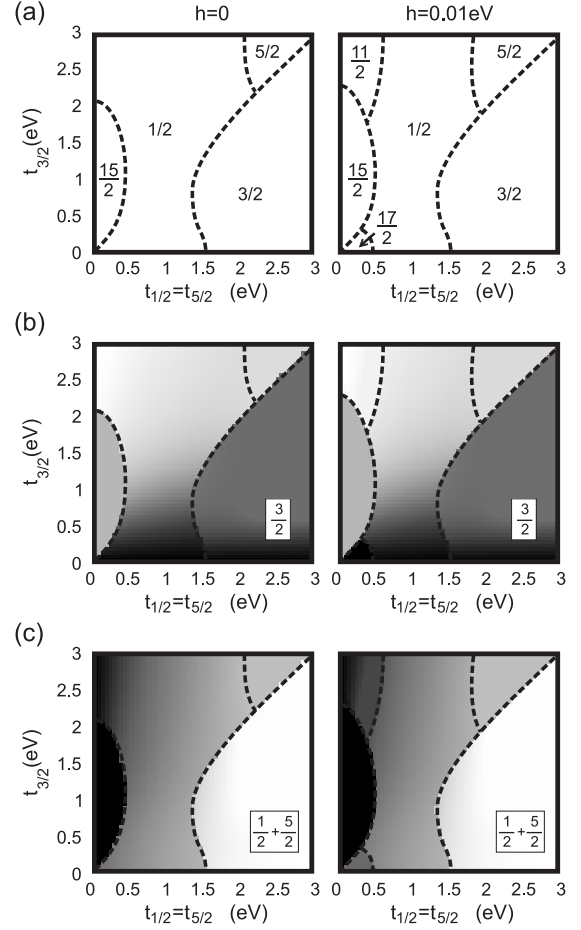

FIG. 8: Phase diagram for the Gutzwiller wavefunction in the $t_{1/2}$-$t_{3/2}$ plane (with $t_{1/2} = t_{5/2}$) for vanishing (left) and finite (right) ferromagnetic field. (a) Phases are characterized by their $\mathcal{J}_z$ expectation value. (b) Ratio $T_{3/2}/t_{3/2}$ as gray-scale plots (black: 0, white: 1.4) and (c) the sum of the corresponding ratios for $j_z = 1/2$ and $5/2$ (black: 0, white: 2.4). In comparison with Fig. 2, note the different plot ranges.

A. Partial localization

In Fig. 8b and 8c, we study the quantity T_{j_z}/t_{j_z} for the Gutzwiller type ansatz (17). If either $t_{3/2} \gg t_{1/2}$ or $t_{1/2} \gg t_{3/2}$, we find again a clear suppression of the non-dominant hopping. It is interesting that in the $\mathcal{J}_z = 1/2$ phase one can go from one case to the other without crossing a phase boundary. This is interesting in so far as a Gutzwiller wavefunction describes this important point without having to introduce phase transitions by symmetry breaking.

VI. SUMMARY AND OUTLOOK

We have studied the interplay and competition of intra-atomic correlations and an anisotropic kinetic energy op-
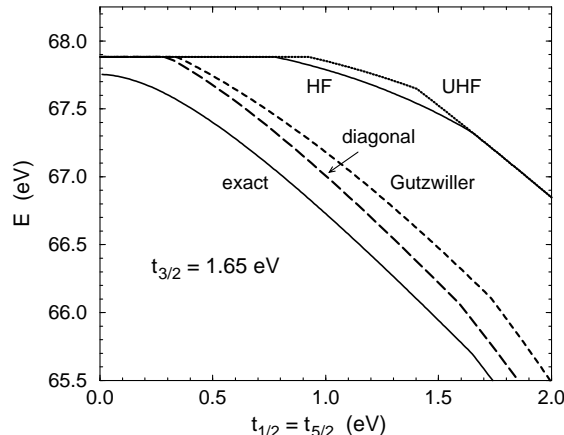
FIG. 9: Total energies for various approximation as function of $t_{1/2} = t_{5/2}$ at fixed $t_{3/2} = 1.65\,\text{eV}$: (exact) numerical diagonalization of the 600×600 matrix, see Fig. 1; (diagonal) diagonalization keeping only the diagonal interaction matrix elements, see Fig. 2; (HF) Hartree Fock approximation, see Fig. 3; (UHF) Unrestricted Hartree Fock approximation, see Fig. 7; (Gutzwiller) variational wavefunction (17), see Fig. 8.

erator by applying three different approximative many-body treatments to the model of Ref. 14. None of them leads to fully satisfactory results. But, the diagonal approximation inspired by the LDA+U approach, i.e. keeping only the matrix elements (6), gives a reasonable good phase diagram with most important phases of the exact solutions being present. This finding should encourage further applications of LDA+U and related approaches such as SIC-LDA for groundstate properties of actinide heavy-fermion materials. We mentioned already in the introduction that some LDA+U calculations indeed show partial localization. However, one can not expect to reproduce within these schemes the small energy scale responsible for the heavy-fermion character of the low-energy excitations.

The numerically easier UHF approximation with j_z-diagonal orbitals agrees quite well with the result of the most general HF ansatz. However, both yield phase diagrams with only weak resemblance with the one from the exact calculation. The substantial suppression of the subdominant hopping found in Fig. 6 might be somehow fortituous.

These observations are confirmed by the total energies given in Fig. 9 for all approximation schemes along a line

$t_{3/2} = 1.65\,\text{eV}$ in the $t_{1/2}$-$t_{3/2}$ plane. The particular $t_{3/2}$ value was chosen such that a large number of phase boundaries is crossed. Clearly, at some phase boundaries kinks of the total energy are seen (related to level crossings) whereas at others higher derivatives change more or less discontinuously (avoided crossings).

We note again that for the exact numerical diagonalization and for the calculation keeping only state-diagonal interaction matrix elements we surpressed configurations f^n with $n \neq 2, 3$, i.e., we worked in the 600 dimensional space rather than the 792 dimensional space. Giving up these restrictions lowers the corresponding energies slightly (not shown).

All curves, except that of the exact solution start with the same value which is constant for a certain range of $t_{1/2}$ and $t_{5/2}$ values. The corresponding wavefunction is the Slater determinant $|\Psi\rangle_{15/2}$, Eq. (13), which completely surpresses $t_{1/2}$ and $t_{5/2}$ hopping. In contrast, the exact ground state near $t_{3/2} = 1.65\,\text{eV}$, $t_{1/2} = t_{5/2} = 0\,\text{eV}$ is not $|\Psi\rangle_{15/2}$, but has intermediate angular momentum $\mathcal{J}_z = 5/2$ and gains energy from all hopping processes. This explains the lower energy and its dependence on all hopping matrix elements.

The solutions of the most general Hartree-Fock scheme (HF) and the case where the single-particle orbitals were restricted to be diagonal with respect to j_z (UHF) differ only in small parts of the parameter space.

While the present model was developed with actinide-based materials in mind, it seems worthwhile to examine the role of intra-atomic correlations in other materials, most noticeable in transition metal compounds.

In conclusion, we find the solutions for the modified Hamiltonian containing the diagonal matrix elements only and the expectation value of the original Hamiltonian with generalized Gutzwiller variational wave function (17) are quite close, because both approaches effectively reduce charge fluctuations but do not include angular correlations equally well. The subtle angular correlations which determine the magnetic character are accounted for only in limiting cases.

VII.   ACKNOWLEDGMENTS

* Present address: Inst. Theoretische Physik, Technische Universität, 01062 Dresden, Germany

[1] J. Schoenes, O. Vogt, J. Löhle, F. Hulliger, and K. Mattenberger, Phys. Rev. B **53**, 14 987 (1996).

[2] T.Takahashi, N. Sato, T. Yokoya, A. Chainani, T. Morimoto, and T. Komatsubara, J. Phys. Soc. Japan **65**, 156 (1995).

[3] N. Metoki, Y. Haga, Y. Koike, and Y. Onuki, Phys. Rev. Lett. **80**, 5417 (1998).

[4] N. Bernhoeft, N. Sato, B. Roessli, N. Aso, A. Hiess, G.H. Lander, Y. Endoh, and T. Komatsubara, Phys. Rev. Lett. **81**, 4244 (1998).

[5] A. Yaouanc, P. Dalmas de Réotier, P.C.M. Gubbens, C.T. Kaiser, A.A. Menovsky, M. Mihalik, and S.P. Cottrell, Phys. Rev. Lett. **89**, 147001 (2002).

[6] M. Dressel, N. Kasper, K. Petukhov, B. Gorshunov, G. Grüner, M. Huth, and H. Adrian, Phys. Rev. Lett. **88**, 186404 (2002).

[7] N.K. Sato, N. Aso, K. Miyake, R. Shiina, P. Thalmeier, G. Varelogiannis, C. Geibel, F. Steglich, P. Fulde, and T. Komatsubara, Nature **410**, 240 (2001).

[8] G. Zwicknagl, A. N. Yaresko, and P. Fulde, Phys. Rev. B **65**, 081103 (2002).

[9] L. Petit, A. Svane, W.M. Temmerman, Z. Szotek, Phys. Rev. Lett **88**, 216403 (2002).

[10] L. Petit, A. Svane, W.M. Temmerman, Z. Szotek, R. Tyer, Euro. Phys. Lett. **62**, 391 (2003).

[11] G. Zwicknagl, A. Yaresko, and P. Fulde, Phys. Rev. B **68**, 052508 (2003).

[12] G. Zwicknagl and P. Fulde, J. Phys.: Cond. Matter **15**, S 1911 (2003).

[13] A.N. Yaresko, V.N. Antonov, and P. Fulde, Phys. Rev. B **67**, 155103 (2003).

[14] D. Efremov, N. Hasselmann, E. Runge, P. Fulde, and G. Zwicknagl, `cond-mat/0303441`, accepted by Phys. Rev. B.

[15] T. Hotta and K. Ueda, Phys. Rev. B **67**, 104518 (2003).

[16] V.I. Anisimov, J. Zaanen, and O.K. Andersen, Phys. Rev. B **44**, 943 (1991).

[17] A. Zunger, J.P. Perdew, and G.L. Oliver, Solid State Commun. **34**, 933 (1980).

[18] P. Strange, A. Svane, W.M. Temmerman, Z. Szotek, and H. Winter, Nature **399**, 756 (1999).

[19] Four-site models have been studied by Frank Pollmann (TU Braunschweig) et al., unpublished.

[20] F. Gebhard, *The Mott Metal-Insulator Transition - Models and Methods*, Springer Tracts in Modern Physics 137, (Springer, Heidelberg, 1997).

[21] M.C. Gutzwiller, Phys. Rev. Lett **10**, 159 (1963).

[22] see, e.g., E.K.U. Gross, E. Runge, and O. Heinonen, *Many-Particle Theory* (Adam Hilger, Bristol, 1991).